REINFORCEMENT METHOD WITH NON-UNIFORM QUANTIFICATION AND EXPERT KNOWLEDGE FOR SMALL SAMPLE SIZE PROBLEM IN TRACK IRREGULARITY FAULT DIAGNOSIS

Zhenghui LI[1*], Na ZHANG[2]

Data-driven intelligent fault diagnosis has achieved significant advancements, garnering increasing interest within the field. Existing data-driven methods generally assume the availability of sufficient fault samples across various severity levels. In the electrical and mechanical engineering field, it is a common problem that high-level fault is difficult to be accurately judged by the fault diagnosis model due to small sample size of high-level fault. This paper proposes a novel approach for track irregularity fault diagnosis addressing this small sample challenge, leveraging reinforcement method with non-uniform quantization and expert knowledge. Initially, a data-driven neural network extracts features from a comprehensive set of fault samples to establish a diagnostic model. Subsequently, targeting the limited high-level fault data, a reinforcement strategy is formulated, integrating non-uniform quantized reliability and Belief Rule Base (BRB) inference. This strategy reinforces the neural network's output layer, enhancing diagnostic sensitivity for small samples and mitigating the risk of high-level fault misdiagnosis, which could adversely impact train operations. Finally, in data experiment on existing railway trunk lines, 9428 sets of railway track vertical irregularity level I-III samples are selected. Compared with support vector machine (SVM) and backpropagation neural network (BP) methods, this method can improve the diagnostic accuracy of vertical irregularity level II-III samples by more than 90%.

Keywords: Track irregularity; Non-uniform quantification; Data driven; Belief rule base; Reinforcement method

1. Introduction

The rapid development of China's railway network has led to increased train speeds, higher carrying capacities, and more frequent departures. As a critical component of this infrastructure, railway track failures significantly impact operational efficiency and safety [1]. Rail is susceptible to geometric deformation, particularly vertical irregularity, due to a confluence of factors. These include inherent impurities from the forging process, uneven subgrade settlement, chemical

[1] Prof., Electrical Engineering, Zhengzhou Railway Vocational & Technical College, Zhengzhou, China, e-mail: 15858190140@163.com
[2] PhD, Electrical Engineering, Zhengzhou Railway Vocational & Technical College, Zhengzhou, China, e-mail: zhangna@zzrvtc.edu.cn

erosion from the environment, and the stresses of heavy train loads and high-frequency rolling [2]. Vertical irregularity, defined as the vertical deviation of the track surface from the ideal rail plane [3], can compromise safety and passenger comfort. Small irregularities amplify locomotive vibrations, while larger irregularities generate substantial impact forces between the wheelset and rail. This can exacerbate track deformation, jeopardizing train safety and potentially leading to derailments [4].

In recent years, monitoring railway track vertical irregularities using in-service vehicles has gained significant attention [5,6]. While still under development, in-service vehicle-based track irregularity measurement systems have emerged globally. These systems often detect various track vertical irregularity faults by measuring bogie acceleration. For instance, Guo et al. demonstrated the monitoring of track irregularities using sensors mounted on bogies [7]. Vibration-based methods analyze the abnormal vibrations of axles, carriages, and bogies induced by track irregularities, correlating these vibrations with specific fault types [8-10]. This method can not only realize real-time fault detection, but also increase the range of railway lines covered by detection, without occupying the running time of railway lines.

The acquisition of vibration data is hampered by interference from vehicle body vibrations and external noise stemming from varying track conditions. Furthermore, sensor inaccuracies introduce additional noise into the acquired vibration signal, obscuring the nonlinear and uncertain relationship between vibration data and track irregularities. While existing information processing methods can detect track irregularities [11,12], the presence of this noise limits their ability to accurately estimate the amplitude and severity of the faults. Recently, data-driven intelligent fault diagnosis methods have shown considerable promise due to their strong feature learning capabilities [13], attracting increasing attention in the field. These methods, including back propagation neural networks (BP) [14] and support vector machines (SVM) [15], are not constrained by model assumptions. However, both statistically and from a model training perspective, data-driven approaches necessitate large amounts of historical track data, a challenge common throughout the industry [13]. The balance of collected samples used to monitor irregularities and wheel wear may impact the robustness of data-driven methodologies. However, for railway track, the number of high-level track irregularity fault sample is often small. It is very accurate for low-level track irregularity fault diagnosis with large sample size, but insensitive for high-level irregularity fault diagnosis with small sample size, and the high-level fault is more harmful to the train. Some scholars have also attempted to use the knowledge representation and reasoning abilities of expert systems to achieve small sample size fault diagnosis. Ming et al. [16] optimized the initial parameters of the Belief Rule Base (BRB) using the Whale Optimization Algorithm (WOA) to achieve fault

diagnosis of the flywheel system. Cheng et al. [17] proposed a BRB-based effective fault diagnosis model for high-speed trains running gear systems,and quantified weight parameters as static reliability and dynamic reliability of attributes in BRB. However, the above method only focuses on optimizing the weight parameters of the antecedent referential point of BRB, without considering the impact of the actual distribution of antecedent referential point on the reference point interval and reliability. Therefore, the non-uniform quantization reliability strategy proposed in this article divides and evaluates the reference point interval and reliability based on the non-uniformity of the actual distribution of antecedent referential point, which can further refine the expert system's characterization of input sample features. This strategy also has strong application value. Moreover, if the input data of BRB is too much, the number of combination rule will increase explosively, which seriously affects the real-time performance of fault diagnosis. Therefore, it is difficult to diagnose high-level small samples submerged in a large amount of data solely using expert systems.

To attack these above problems, this proposed method integrates the interpretability of expert systems for small sample analysis with the feature learning capabilities of data-driven methods typically employed with larger datasets. The neural network model is used to model a large number of low-level and high-level fault samples, while the BRB model is used to model a small number of high-level fault samples and design non-uniform quantization strategy to consider impact of the actual distribution of antecedent referential point on the reference point interval and reliability. The BRB model with non-uniform quantization strategy is used to reinforce the neural network's output layer, enhancing diagnostic sensitivity for small samples and mitigating the risk of high-level fault misdiagnosis. This enhances the diagnostic performance of data-driven approaches, mitigating their sensitivity to limited data. Given the scarcity and critical importance of high-level fault data, maximizing its utilization is paramount, aligning with the principle of judicious resource allocation.

2. Reinforcement strategy with data-driven model and expert knowledge system

2.1. Data collection and pre-processing

$f_1(t)$and $f_2(t)$ as input sample sets for fault diagnosis models, I= {[$f_1(t), f_2(t)$] | t=1, 2,…, T}. $\tilde{I} = \{[\tilde{f}_1(t), \tilde{f}_2(t)] \mid t = 1, 2, \ldots, \tilde{T}\}, \tilde{I} \in I$ is the high-level input sample set with small size. $Ir(t)$ as the output sample set of the fault diagnosis model, O={[$Ir(t)$]| t=1, 2,…, T}. Normalize the original input and output samples, and map the input and output sample features to [-1,1]. The normalization formula is :

$$f(t)^* = \left[\frac{f(t) - f(t)_{\min}}{f(t)_{\max} - f(t)_{\min}} \times 2 \right] - 1 \tag{1}$$

The normalized model input is $I^*=\{[f_1(t)^*, f_2(t)^*] | t=1, 2,\ldots, T\}$.The normalized model output is $O^*=\{[Ir(t)^*] | t=1, 2,\ldots, T\}$.

2.2. Data-driven fault diagnosis model

Backpropagation (BP) is a prominent supervised learning algorithm for artificial neural networks (ANNs). The system learns by computing the error in the output layer and subsequently propagating this error backward to adjust the weights of the hidden layers. This backpropagation of error makes it particularly well-suited for modeling nonlinear relationships between inputs and outputs (see Fig. 1).

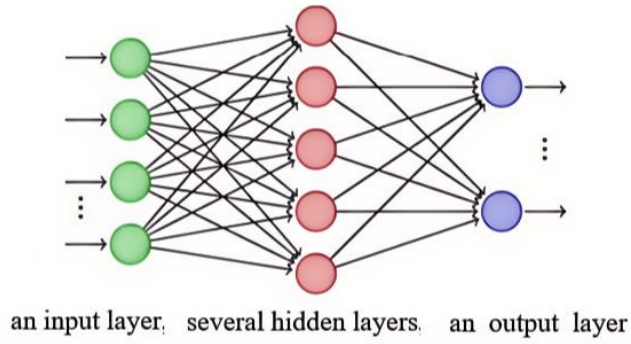

Fig. 1. The structure diagram of BP neural network

The sigmoid function is used as the activation function for the above model. The purpose of introducing an activation function is to inject nonlinearity into the neural network, thereby enabling it to effectively handle nonlinear problems. Without an activation function, the neural network would remain purely linear. The sigmoid function performs well when used for classifiers, and its expression is:

$$f(x)=1/(1+e^{-x}) \tag{2}$$

Gradient descent is employed to optimize the network weights by minimizing the output error. This principle is expressed as:

$$E_p = \sum_{t=1}^{T} (O_o(t)^* - y_o(t))^2 \tag{3}$$

where $O_o(t)^*$ and $y_o(t)$ represent the actual sample output and the output value of the t-th unit, respectively. P denotes the p-th pattern; T is the number of the output units. The gradient descent update rule is given by Equation 4.

$$w_{kt} = -\mu \frac{\partial E_p}{\partial w_{kt}} \tag{4}$$

w_{kt} is the weight of the t^{th} unit in the $(n\text{-}1)^{th}$ layer to the k^{th} unit in the nth layer.The BP calculates errors in the output layer ∂_l, and the hidden layer ∂_j are using the formulas in Equation 5.

$$\begin{aligned} \partial_l &= \mu(O_o(t) * -y_o(t)) f'(y_o(t)) \\ \partial_j &= \mu \sum\nolimits_t \partial_t w_{tj} f'(y_o(t)) \end{aligned} \tag{5}$$

The weights w_{tj} and biases b_t are updated according to the equations:

$$\begin{aligned} w_{tj}(k+1) &= wt_j(k) + \mu \partial_j y_o(t) \\ w_{lj}(k+1) &= wl_j(k) + \mu \partial_j x_l \\ b_t(k+1) &= b_t(k) + \mu \partial_j \end{aligned} \tag{6}$$

Here, k is the number of the epoch and μ is the learning rate. According to the trained BP network model, the estimated value of model output is $O' = \{[\, Ir(t)' \,] | \, t=1, 2,\ldots, T\}$.The actual track irregularity amplitude is $O=\{[Ir(t)] | \, t=1, 2,\cdots, T\}$.The output layer error of the model is defined as *Err*.

2.3. Reinforcement strategy

Although the above data-driven model can diagnose fault samples with large amounts of data, it is not sensitive to fault samples with small amounts of data. High level fault samples are usually small in data size. Therefore, the data-driven model has low ability to diagnose high-level faults. Therefore, a reinforcement model based on belief rule base reasoning is constructed by using section (2.1) high level fault data set $\bar{I} = \{[\bar{f}_1(t), \bar{f}_2(t)] \,|\, t = 1,\ 2, \ldots, \bar{T}\}$ and section (2.2) model output layer error *Err*, combined with the idea of non-uniform quantization, to reinforce the output layer of BP network model based on data-driven. The workflow is illustrated in Fig. 2, with detailed steps outlined below.

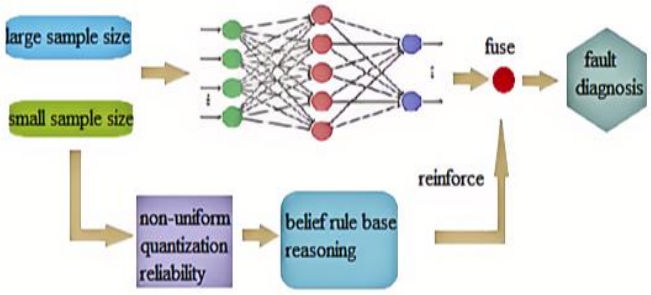

Fig. 2. The flow diagram of reinforcement strategy

The BRB methodology utilizes an extended if-then rule structure to represent diverse forms of uncertain information and knowledge. The parameters within the BRB system (e.g., attribute values and weights, belief distributions, and

rule weights) possess clear physical interpretations, readily understood by both domain experts and users. Consequently, BRB demonstrates a strong capacity for approximating complex nonlinear causal relationships across a broad range of applications.

The belief rules are developed using accumulated data and insights from track irregularity experiments. These rules incorporate antecedent attributes $\tilde{f}_1(t), \tilde{f}_2(t)$ and the consequences (the belief distributions about *Err*). The concept of BRB construction and the importance of model parameters are outlined in Table 1.

In Table 1, the *k*-th belief rule R_k is represented as:

If $\tilde{f}_1(t) = A_1^k$ and $\tilde{f}_2(t) = A_2^k$, then $Err = \{(D_1,\beta_{k,1}), \ldots,(D_m, \beta_{k,m})\}$,

$$\sum_{j=1}^{m} \beta_{k,j} = 1,\ k=1, 2, \ldots,L. \tag{7}$$

Table 1

The idea of BRB construction and the significance of model parameter

BRB system	significance of model parameter
the referential point set of the antecedent attribute $A_i^k = \{A_i^k \mid i = 1,2\ , k = 1,2, \ldots, L\}$	input variables $\tilde{I} = \{[\tilde{f}_1(t), \tilde{f}_2(t)] \mid t = 1,\ 2,\ \ldots, \tilde{T}\}$
the consequent attribute of R_k: $\{(D_1,\beta_{k,1}), \ldots, (D_m, \beta_{k,m})\}$	D_m is the referential value of the consequent attribute, $\beta_{k,m}$ is the belief value of D_m
the weight of the belief rule $\phi_k \in [0,1]$	the relative importance of R_k
the weight of the attribute $\delta_i \in [0,1]$	the relative importance of δ_i

Step (1): A reinforcement model is established to describe the relationship between high-level fault input sample set $\tilde{I} = \{[\tilde{f}_1(t), \tilde{f}_2(t)] \mid t = 1,\ 2,\ldots, \tilde{T}\}$ and BP network model output layer error *Err*. *L* is the total number of rules in the Belief Rule Base, D_m is the referential value of the consequent attribute *Err*, $\beta_{k,j}$ is the belief degree to which D_m is believed to be the consequent when $\tilde{f}_1(t) = A_1^k \wedge \tilde{f}_2(t) = A_2^k$. At the same time, attribute weight of $\tilde{f}_1(t)$, $\tilde{f}_2(t)$ is initialized to δ_I=0.5, δ_{II}=0.5 ,and their rule weight is all set to 1.

Step (2): Because the track is often in complex environment such as vibration disturbance of train operation and wheel-pair repeated rolling, the spatial distribution of fault input $\tilde{f}_1(t)$ and $\tilde{f}_2(t)$ shows strong discreteness and heterogeneity. Therefore, the referential point of $\tilde{f}_1(t)$ and $\tilde{f}_2(t)$ is processed with the idea of non-uniform quantization, which makes the reference point more refined

to characterize the characteristics of input samples. The non-uniform quantization reliability of A_1^k is $\xi_1^k = \left\{ \xi_{1,1}^k, \xi_{1,2}^k, \cdots, \xi_{1,q}^k \right\}$. The non-uniform quantization reliability of A_2^k is $\xi_2^k = \left\{ \xi_{2,1}^k, \xi_{2,2}^k, \cdots, \xi_{2,q}^k \right\}$.

$$\xi_{\tau,\nu}^k = \overline{N} \Big/ \rho \tag{8}$$

$$\rho = \frac{\overline{T}}{q} \tag{9}$$

$\nu = 1, 2, \cdots, q$, τ=1 *or* 2, $\overline{N}$ is the number of the small samples within the range of reference point $A_{\tau,\nu}^k$, $\overline{T}$ is the number of the small samples. When $\nu = 1$, the range of this reference point is $\left[A_{\tau,1}^k, \frac{A_{\tau,2}^k - A_{\tau,1}^k}{2} \right]$, when $\nu = q$, the range of this reference point is $\left[\frac{A_{\tau,q}^k - A_{\tau,q-1}^k}{2}, A_{\tau,q}^k \right]$, when $q > \nu > 1$, the range of this reference point is $\left[\frac{A_{\tau,\nu}^k - A_{\tau,\nu-1}^k}{2}, \frac{A_{\tau,\nu+1}^k - A_{\tau,\nu}^k}{2} \right]$.

Step (3): On the basis of reinforcement model in step (2), when the error result of the output layer is calculated by the BP neural network in step (1), $f_1(t)$ and $f_2(t)$ will be input into the reinforcement model base on the belief rule base. $f_1(t)$ and $f_2(t)$ will match the reference point A_τ^k(τ=1 *or* 2) of the antecedent attribute in varying degrees, and the matching degree is α_τ^k. If $f_\tau(t)$ is greater than reference point $A_{\tau,q}^k$, its matching degree to $A_{\tau,q}^k$ is 1; If $f_\tau(t)$ is less than reference point $A_{\tau,1}^k$, its matching degree to $A_{\tau,1}^k$ is 1. If $A_{\tau,1}^k \le f_\tau(t) \le A_{\tau,q}^k$, its matching degree α_τ^k to the corresponding reference point is calculated as follows:

$$\alpha_{\tau,\nu}^k = \left[(A_{\tau,\nu}^k - f_\tau(t)) / (A_{\tau,\nu}^k - A_{\tau,\nu\text{-}1}^k) \right] \times \xi_{\tau,\nu}^k, \tag{10}$$

$$\alpha_{\tau,\nu\text{-}1}^k = (f_\tau(t) - A_{\tau,\nu}^k) / (A_{\tau,\nu}^k - A_{\tau,\nu\text{-}1}^k) \times \xi_{\tau,\nu\text{-}1}^k. \tag{11}$$

When the antecedent reference point of the belief rule is matched, the corresponding belief rule will be activated. The weight φ_k of the activated rule is updated as follows:

$$\varphi_k = \phi_k \prod_{\tau=1}^{H} (\alpha_\tau^k)^{\bar{\delta}_\tau} \Bigg/ \sum_{k=1}^{T} \left[\phi_k \prod_{\tau=1}^{H} (\alpha_\tau^k)^{\bar{\delta}_\tau} \right], \tag{12}$$

where $\phi_k \in [0,1]$ is the weight of belief rules, H is the number of input variables, $\bar{\delta}_\tau$ is the relative attribute weight of the activated rule:

$$\bar{\delta}_\tau = \delta_\tau \Big/ \max_{\tau=1,2,\ldots H} \{\delta_\tau\}. \tag{13}$$

According to the above calculated φ_k and α_τ^k, the consequent attribute of the activated rule is fused using the evidential reasoning theory, and the reinforcement result Err' is calculated as follows:

$$Err'(f_1(t), f_2(t)) = \{(D_j, \beta_j), j = 1,2,\cdots,m\}, \tag{14}$$

where

$$\beta_j = \frac{\varepsilon \left[\prod_{k=1}^{L} (\varphi_k \beta_{k,j} + 1 - \varphi_k \sum_{k=1}^{m} \beta_{k,j}) - \prod_{k=1}^{L} (1 - \varphi_k \sum_{j=1}^{m} \beta_{k,j}) \right]}{1 - \varepsilon [\prod_{k=1}^{L} (1 - \varphi_k)]}, \tag{15}$$

$$\varepsilon = \left[\sum_{j=1}^{m} \prod_{k=1}^{L} (\varphi_k \beta_{k,j} + 1 - \varphi_k \sum_{j=1}^{m} \beta_{k,j}) - (m-1) \prod_{k=1}^{L} \left(1 - \varphi_k \sum_{j=1}^{m} \beta_{k,j} \right) \right]^{-1} \tag{16}$$

β_j represents the belief level of the j-th subsequent attribute, $\beta_{k,j}$ express the belief distribution of the j-th subsequent attribute in the k-th belief rule. The final prediction value O of track vertical irregularity can be calculated by adding the prediction value O' in step (1) and the reinforcement value Err'.

3. The setting and diagnosis result analysis of experiments

3.1. Training database built

(1) Collect vibration data of track vertical irregularity

According to the principle based on the vibration analysis method and the analysis of the detection data obtained, a clear relationship exists between track irregularity amplitude and vibration signals, as evidenced by the vibration data collected at both carriage and axle positions [4]. The empirical data consist of track irregularity measurements, axle acceleration sensor data, and carriage acceleration sensor data collected by track inspection vehicles over the downline section (1584.5103 km to 1586.86735 km) of China's existing railway trunk lines [18]. The track inspection vehicle runs at the speed of 100km/h and collects the relevant parameter signals of the track every 0.25m. So the time step is t=1,...,T, where T is

the total number of samples and T=((1586.86735-1584.5103)/0.25)$\times 10^3$=9428. The acquired original vibration data in time-domain is shown in Fig. 3. r represents the amplitude of the track's vertical irregularity, f_1 and f_2 denote the vibration data of the axle and the carriage.

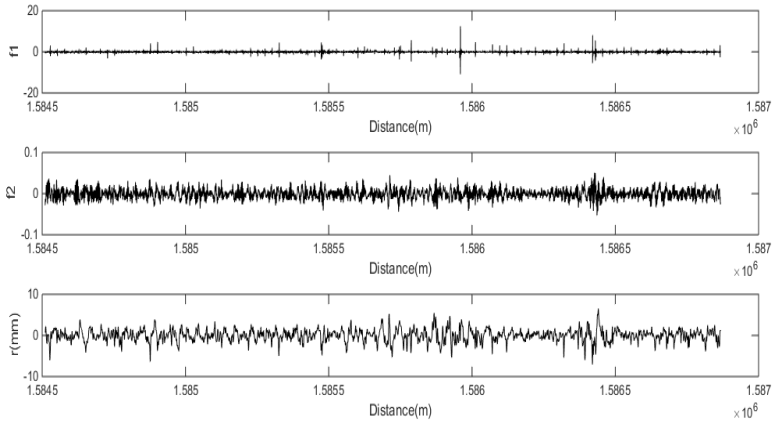

Fig.3. The acquired original vibration data

(2) Pre-processing of training data

At each time step, we use the short-time Fourier transform to obtain the absolute mean values of the frequency amplitudes of f_1 and f_2 with a window size of 5.25m, respectively denoted as $f_1(t)$ and $f_2(t)$, $Ir(t)$ represents the absolute value of r, as illustrated in Fig. 4.

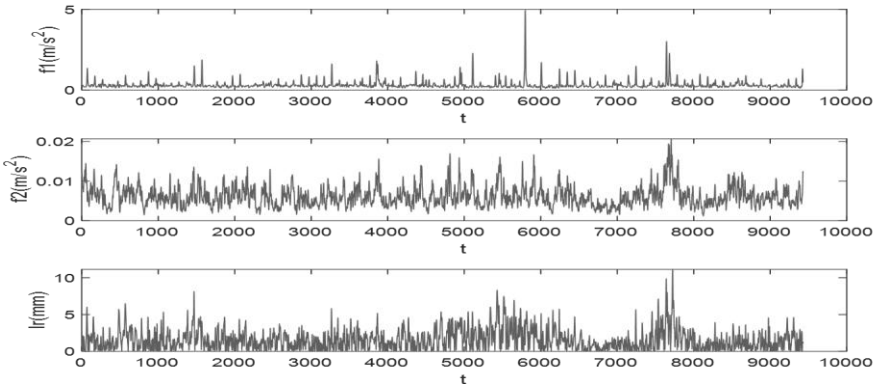

Fig.4. The absolute mean values $f_1(t)$, $f_2(t)$ and the absolute value $Ir(t)$

Although the relationship between $f_1(t)$, f_2 (t) and $Ir(t)$ is nonlinear, there is some correlation in the trend of changes between $f_1(t)$, f_2 (t) and $Ir(t)$. To demonstrate the correlation between $f_1(t)$, f_2 $(t)$and $Ir(t)$, we conducted an analysis

from both physical theory and data analysis perspectives. 1. In terms of physical theory.When the magnitude of track irregularities changes rapidly, the axle acceleration sensor data is more sensitive, whereas when the magnitude is larger, the carriage acceleration sensor data becomes more sensitive. To accurately estimate the level of vertical irregularity, it is essential to integrate the acceleration vibration data from both the axle and the carriage. 2. In terms of data analysis. For example, in the sample intervals of 1000-2000, 5500-6000, and 7500-8500, as the amplitude of railway track vertical irregularity increases, the vibration amplitude of the axle and carriage also increases. In the sample interval of 6500-7000, as the amplitude of railway track vertical irregularity decreases, the vibration amplitude of axle and carriage also decreases.According to relevant regulations [19], the level of vertical irregularity of the track in railway track defects is defined in Table 2.

Table 2

The vertical irregularity levels of track

(160 km/h~200 km/h)	Acceptance	Discomfort	Temporary repair	Speed limit
Level	I	II	III	IV
Standard(mm)	$0 \le Ir \le 5$	$5 < Ir \le 8$	$8 < Ir \le 12$	$12 < Ir$

3.2. Data-driven fault diagnosis model

Based on the analysis of track vertical irregularity sample data, a neural network was configured with six layers: one input layer, four hidden layers, and one output layer. The network underwent 5000 training iterations with a training accuracy threshold of 0.00001 and a learning rate of 0.01. According to the formula in Section 3, 9428 groups of ($f_1(t)$), ($f_2(t)$), and ($Ir(t)$) were input into the network for model training.Based on the prediction result $O' = \{[\, Ir(t)' \,] \mid t=1, 2,\ldots, T\}$ of the BP network model and the true value $O=\{[Ir(t)] \mid t=1, 2,\ldots, T\}$ of the track vertical irregularity amplitude, the prediction error of the model output layer is calculated as *Err*. For 9428 groups of $f_1(t)$ 、 $f_2(t)$, the prediction result error is [2.0703,1.9627,1.5156,0.9646,0.5041,0.1668, ..., 0.0185,0.0197], and the root mean square error of the error is 1.2840. The diagnostic accuracy for 9,201 groups at irregularity level I is 99.9%, with 9,195 groups correctly diagnosed. For the 207 groups exhibiting irregularity at level II, the diagnostic accuracy is 2.4%, with only five groups accurately identified. For 21 groups with track vertical irregularity at level III, the diagnostic accuracy is 0%, with no groups accurately identified. This indicates that the accuracy of the BP network model is insufficient for high-level faults. Therefore, integrating expert knowledge from small sample theory is necessary to enhance its compensatory capabilities.

3.3. Reinforcement strategy

To address the limitations of the aforementioned fault diagnosis model in effectively diagnosing level II and level III fault data, a reinforcement model has been developed. This model aims to enhance the diagnostic accuracy for these fault levels, particularly when dealing with small sample sizes, by utilizing belief rule base inference. Let level II and level III fault input data set as $\tilde{f}_1(t)$, $\tilde{f}_2(t)$, and the reference points of $\tilde{f}_1(t)$ is [0.129,0.2,0.25,0.8,1,1.25, 3.015], the non-uniform reliability of the above reference points is calculated as [0.7, 0.8, 0.65, 0.8, 0.5, 0.75, 0.85] by the formula in section 2.3. Similarly, the reference points of $\tilde{f}_2(t)$ is [0.0026,0.005,0.006,0.008,0.0111,0.015,0.0167], the non-uniform reliability of the above reference points is calculated as [0.9,0.6,0.8,0.8,0.7,0.85,0.5] by the formula in section 2.3. The reference points of *Err* is [0.04, 0.45, 1, 1.5, 2.1, 6.02], some belief rules constructed by expert knowledge are shown in Table 3. The specific fusion reasoning process is as follows:

Table 3

Some belief rules of the belief rule base

No	θ_k	$\tilde{f}_1(t)$ & $\tilde{f}_2(t)$	*Err*					
			β_1	β_2	β_3	β_4	B_5	B_6
1	1.0	VS & VS	0	0	0	0	0.6403	0.3597
⋮	⋮	⋮	⋮	⋮	⋮	⋮	⋮	⋮
15	1.0	VS & VL	1	0	0	0	0	0
⋮	⋮	⋮	⋮	⋮	⋮	⋮	⋮	⋮
25	1.0	PM & VL	0	0	0	0	0.5906	0.4094
⋮	⋮	⋮	⋮	⋮	⋮	⋮	⋮	⋮
35	1.0	PM & PS	0	0	0.3900	0.610	0	0
⋮	⋮	⋮	⋮	⋮	⋮	⋮	⋮	⋮
49	1.0	VL & VL	0	0.0455	0.9545	0	0	0

Step (1): Calculate the matching degree of input parameters

In this study, $f_1(t)$ and $f_2(t)$ are utilized as inputs for the reinforcement model. The model calculates the matching degree of each fault characteristic data group relative to their respective reference points, A_1^k and A_2^k, using equations (9) and (10) in Section 2.3. For example, when the 5737-th group of feature data is input, the input parameter is [0.1710, 0.0051], the matching degree between $f_1(t)$ and reference points [0.129,0.2] is 0.2856,0.4737, the matching degree between $f_2(t)$ and reference points [0.005,0.006] is 0.5303,0.0930.

Step (2): Calculate the weight of the activated rule

After obtaining the matching degree α_i^k of the input data to the reference point in each rule, calculate the weight φ_k of the activated rule using formulas (12) and (13). For example, for the 5737-th group of feature data, we can get the activation weight of some belief rules (R_2, R_3, R_9, R_{10}) is φ_2=0.3605, φ_3=0.0474, φ_9=0.5233 and φ_{10}=0.0688 respectively, while the activation weight of other rules is all 0, four belief rules are activated.

Step (3): Fusion mechanism of activated rule

The fused output belief structure $Err'(f_1(t), f_2(t)) = \{(D_j, \beta_j), j = 1, 2, \cdots, 6\}$ is obtained by using evidential reasoning theory, where D_j and β_j can be calculated by formula (15) and formula (16) respectively. For example, bring φ_k and $\beta_{k,j}$ of the 5737-th group of characteristic data into formula (14), $Err'(f_1(t), f_2(t)) = \{(D_1, 0.0266), (D_2, 0), (D_3, 0), (D_4, 0), (D_5, 0.4514), (D_6, 0.7178)\}$. Finally, the error compensation estimate Err'=1.1958.

Step (4): Analysis of experimental result

The above 5737-th group of data is substituted into the calculation, and the predicted value (O'=4.5064) of track irregularity amplitude obtained by the neural network model, plus the error reinforcement estimated value (Err'=1.1958) calculated by the reinforcement model, the final track irregularity amplitude estimated value $O = O' + Err'$=4.5064+1.1958=5.7022mm. This method can compensate the sample which is misjudged as track vertical irregularity fault level I to track vertical irregularity fault level II.

3.4. Diagnosis result analysis

The confusion matrix of diagnostic results is depicted in Table 4. Each column of the confusion matrix represents the predicted value (unbolded number), and each row represents the actual category (bolded number). The results of the proposed method are highlighted in bold, whereas the results of the BP method are indicated in regular font with numbers in parentheses. The data-driven BP method maintains high sensitivity for large samples but lacks sensitivity for small samples. Due to the limited data, the data-driven model incorrectly assumes that small samples are insignificant during the training process. Among 207 sets of irregularity level II samples, this method misdiagnosed 200 sets as irregularity level I samples. The proposed method achieves a diagnostic accuracy of 99.9% (9196 sets correct) for 9201 sets of irregularity level I samples. For 207 sets of irregularity level II samples, the diagnostic accuracy improves to 96.6% (200 sets correct). For 20 sets of irregularity level III samples, the diagnostic accuracy increases to 90.0% (19 sets correct). This proposed method integrates the interpretability of expert systems for small sample processing with the feature learning ability of data-driven methods for

large samples, enhancing the diagnostic capacity of data-driven methods for small samples.

To further validate the effectiveness of the proposed method, this paper compared the diagnostic performance of the Support Vector Machine (SVM) and Backpropagation (BP) methods on 9428 sets of track irregularity samples at varying levels, as presented in Table 5.

Table 4

The confusion matrix of diagnostic results

The confusion matrix of Data-Driven(BP) method and proposed method					
Track irregularity level	Level I	Level II	Level III	Total	Diagnostic accuracy
Level I	**9196**(9195)	5(4)	0(2)	9201	**99.9%**(99.9%)
Level II	5(202)	**200**(5)	2(0)	207	**96.6%**(2.4%)
Level III	0(15)	2(5)	**18**(0)	20	**90.0%**(0%)

Table 5

The diagnostic accuracy for different levels track irregularity samples

Method	Diagnostic accuracy		
	Level I	Level II	Level III
SVM-test	97.1%	1.5 %	0%
BP-test	99.9%	2.4%	0%
Proposed method	**99.9%**	**96.6%**	**90.0%**

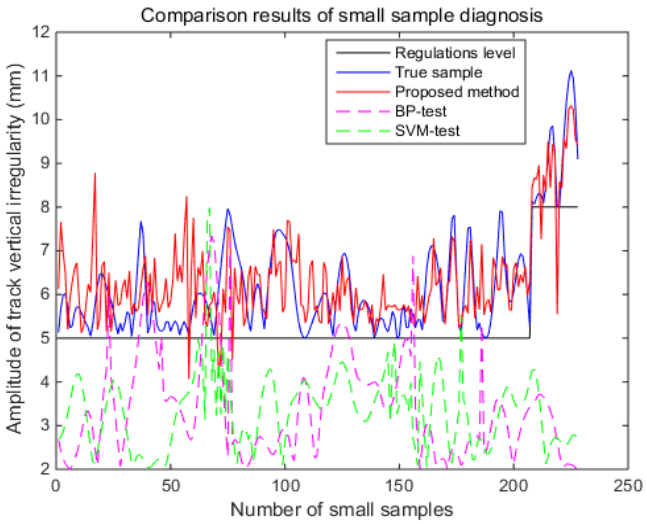

Fig. 5. The diagnostic results for small samples

The diagnostic accuracy of the SVM method for irregularity level I samples is 97.1%, while for level II samples, it is only 1.5%, and for level III samples, it is 0%. Similarly, the BP method achieves a diagnostic accuracy of 99.9% for level I samples, 2.4% for level II samples, and 0% for level III samples. These results

indicate that both SVM and BP methods struggle to accurately diagnose small sample sizes. To enhance the clarity of diagnostic performance comparisons for small samples, this paper categorizes 207 sets of irregularity level II samples and 20 sets of level III samples. The diagnostic results for these small samples are depicted in Fig. 5. This figure illustrates that both SVM and BP methods have difficulty fitting the nonlinear trend of small samples. For the irregularity level III samples, which comprise only 20 data sets, neither method can accurately identify the irregularities. The proposed method effectively fits the nonlinear trend of small samples and enhances diagnostic accuracy for larger samples.

4. Conclusion

The amplitude of track irregularities significantly impacts the train safe operation. A prevalent challenge in diagnosing severe track irregularities is the contradiction between the small sample size and the high risk they pose. Due to the limited samples of severe faults, accurately diagnosing these faults is challenging for traditional models. To address this issue, we propose a reinforcement approach that incorporates non-uniform quantification and expert knowledge to tackle the small sample size problem in track irregularity fault diagnosis. The experimental results demonstrate that expert knowledge systems have significant advantages in diagnosing high-level track irregularities with limited sample sizes, whereas data-driven methods inherently excel in identifying low-level track irregularities when ample samples are available. In industrial electrical and mechanical engineering field, high-level faults occur infrequently, whereas low-level faults are more prevalent. Consequently, data on high-level faults is extremely valuable. Relying solely on data-driven methods for fault diagnosis in these systems can result in the overshadowing of valuable high-level fault data by the abundance of low-level fault data. Importantly, high-level faults are often the most dangerous and destructive. Thus, employing a non-uniform quantization expert knowledge system to enhance data-driven fault diagnosis methods addresses the limitations of accurately identifying faults in small samples. This approach is theoretically significant and offers even greater practical benefits.
Test results indicate that this method holds promise for application in railway engineering.

This paper concludes with several suggestions for future research: (1) The proposed method represents a significant effort to address the small sample size issue in track irregularity fault diagnosis using both data and knowledge. This approach is not confined to data-driven methods like BP or SVM. (2) While the proposed method offers a viable solution for the small sample size problem, exploring state estimation might also be an effective strategy for managing random disturbances.

Acknowledgments

This work was financially supported by Key scientific research projects of colleges and universities in Henan Province (25A580011) and Scientific &Technological Research Project in Henan Province (242102240130).

REFERENCES

[1] *Y. B. Yang, Zhi-Lu Wang, Kang Shi, et al.* State-of-the-Art of Vehicle-Based Methods for Detecting Various Properties of Highway Bridges and Railway Tracks, International Journal of Structural Stability and Dynamics, 20(13), 2020,2041004.

[2] *Odashima, M., Azami, S*. Track geometry estimation of a conventional railway from car-body acceleration measurement, Mech. Eng. J. 4,2017, pp.16-98.

[3] *Li Chenzhong, Qing He.* Estimation of railway track longitudinal irregularity using vehicle response with information compression and Bayesian deep learning. Computer-Aided Civil and Infrastructure Engineering, 37(10),2022, pp: 1260-1276.

[4] *Kairas, T., Berg, M*. Correlation of track irregularities and vehicle responses based on measured data, Veh. Syst. Dyn, 56,2018, pp. 967-981.

[5] *Tsunashima, H., Naganuma, Y*. Track geometry estimation from car-body vibration, Veh. Syst. Dyn, 52(1),2014, pp. 207-219.

[6] *Kairas, T., Berg, M.* Correlation of track irregularities and vehicle responses based on measured data, Veh. Syst. Dyn, 56,2018, pp. 967-981.

[7] *Guo, Fengqi, and Pengjiao Wang*. Measurement and analysis of the longitudinal level irregularity of the track beam in monorail tour-transit systems. Scientific Reports, 12(1), 2022,19219.

[8] *Yang Y L*.Research on relationship between track detection method and line maintenance, Technological Innovation and Productivity, 2,2018, pp.108-110.

[9] *Mori, H., Tsunashima, H., Kojima, T., et al.* Condition monitoring of railway track using in-service vehicle, Journal of Mechanical Systems for Transportation and Logistics, 13(1), 2010, pp.154-165.

[10] *Zhang, Z., Xu, X., Zhang, X*. Intelligent identification for vertical track irregularity based on multi-level evidential reasoning rule model, Appl Intell, 52, 2022, pp. 16555-16571.

[11] *Ning J, Lin JH, Zhang B*, Time-frequency processing of track irregularities in high-speed train, Mech Syst Signal Process, 66,2016, pp. 339-348.

[12] *Bhardwaj B, Bridgelal R, Chia L, Lu P, et al.* Signal filter cut-off frequency determination to enhance the accuracy of rail track irregularity detection and localization, IEEE Sensors, 20(3),2020, pp.1393-1399.

[13] *Hao Su, Ling Xiang*. A novel method based on meta-learning for bearing fault diagnosis with small sample learning under different working conditions, Mechanical Systems and Signal Processing, 169, 2022,108765.

[14] *Ye, Y., Huang, P. and Zhang, Y.* Deep learning-based fault diagnostic network of high-speed train secondary suspension systems for immunity to track irregularities and wheel wear, Rail. Eng. Science, 30,2022, pp.96-116.

[15] *Tsunashima H*. Condition Monitoring of Railway Tracks from Car-Body Vibration Using a Machine Learning Technique, Applied Sciences, 9(13), 2019, pp.27-34.

[16] *Ming Z, Zhou Z*. A new interpretable fault diagnosis method based on belief rule base and probability table, Chinese Journal of Aeronautics, 36(3),2023, pp. 184-201.

[17] *Cheng, Chao.* A BRB-based effective fault diagnosis model for high-speed trains running gear systems, IEEE Transactions on Intelligent Transportation Systems, 23(1), 2020, pp. 110-121.
[18] *Xu XB, Zheng J, Yang JB.* Track irregularity fault identification based on evidence reasoning rule, IEEE International Conference on Intelligent Rail Transportation (ICIRT*)*, 2016, 16378174.
[19] Ministry of Railways of the Peoples Republic of China, Railway Line Repair Rules, Beijing: Chinese Railway Press, 2021.